ISSN-1996-918X

Pak. J. Anal. Environ. Chem. Vol. 23, No. 2 (2022) 237 – 246

http://doi.org/10.21743/pjaec/2022.12.06

Synthesis of Bio-Metal Organic Framework-11 Based Mixed Matrix Membrane for Efficient Carbon Dioxide Separation

Tariq Hussain[1], Zahid Naeem Qaisrani[2,3*], Asadullah[2], Zaman Tahir[4], Ali Nawaz Mengal[5] and Muhammad Sagir[1]

[1]Department of Chemical Engineering, University of Gujrat, Hafiz Hayat Campus, Gujrat, 50700, Pakistan.
[2]Department of Chemical Engineering, Faculty of Engineering & Architecture, Balochistan University of Information Technology, Engineering and Management Sciences (BUITEMS), Takatu Campus, Airport Road Quetta, 87300, Balochistan, Pakistan.
[3]Faculty of Environmental Management, Prince of Songkla University, Hatyai Campus, 90112, Songkhla, Thailand.
[4]Department of Chemical Engineering, COMSATS Institute of Information Technology, Lahore Campus, Lahore, Pakistan.
[5]Department of Mechanical Engineering, Faculty of Engineering & Architecture, Balochistan University of Information Technology, Engineering and Management Sciences (BUITEMS), Takatu Campus, Airport Road Quetta, 87300, Balochistan, Pakistan.
Corresponding Author Email: engr.zbaloch@gmail.com

Received 11 June 2021, Revised 30 November 2022, Accepted 10 December 2022

Abstract

Mixed matrix membranes are thought to have the ability to separate gases. The current research investigates the isolation of CO_2 from methane (CH_4) and nitrogen (N_2) using a mixed matrix membrane. Bio-MOF-11 was combined with polyether sulfone to establish a membrane (PES). Experiments were carried out to determine the efficiency of the established membrane. Results showed that the Lewis basic sites present in Bio-MOF-11, which have a higher affinity for CO_2, increase the permeability and selectivity of pristine polyether sulfone. At 30% filler loading, CO_2 permeability improved from 2.20 to 3.90 Barrer, while CO_2/CH_4 and CO_2/N_2 selectivity improved from 9.57 to 11.14 with 30% filler loading. In addition, at 30% filler loading, CO_2 solubility drops from 1.57 to 1.20.

Keywords: Bio- MOF-11, Membranes, Metal Organic Framework, Poly Ether Sulfone, CO_2 separation.

Introduction

World's Population is continuously increasing and is expected to reach 9.2 billion people by 2050. With a growing population, human demands are increasing and putting extensive pressure on natural resources. Researchers today realized the situation and the world is adopting alternative solutions for the sustainability of resources and energy demands [1–3]. Extensive use of fossil fuels not only depletes resources but has an adverse effect on climate too [4]. Keeping in view the increasing energy demands, switching towards green energy and CO_2 free world is of great concern today [5].

Human activities change the concentration of CO_2 by burning fossil fuels and industrial waste materials. CO_2 is affecting our environment because of its anthropogenic nature causing high uncertainty [4,6,7]. The World Meteorological Organization, in its 2019 report, mentioned

that currently the CO_2 concentration in the atmosphere is 412 parts per million and rising continuously.

To lower down the atmospheric level of greenhouse gases (GHG) and temperature of the globe, three options are being explored which are:

(a) Energy efficiency improvement
(b) Sequestration of Carbon
(c) Useless carbon-intensive energy sources

Hence it is necessary to decrease the concentration of CO_2. Two ways were discussed in the literature to resolve the issue. The first one is to reduce the usage of fossil fuels which is currently not possible, the other is to capture the CO_2 and restore it and use it to make useful products which is a better option [10,11]. There are many techniques to separate CO_2 from gases which include adsorption, absorption, cryogenic distillation, and membranes [12–15]. In this regard, gas separation membranes can help to control environmental pollution by capturing CO_2 from different streams. Initially, membrane usage was limited because of low flux and selectivity. A larger area is required for higher flux, which means capital investment is high, and low selectivity means the operating cost will be high. So, it is desired to explore materials with higher selectivity, high surface area, and better permeation which can also stand against plasticization, aging, and conditioning.

The difference in chemical and physical properties has created a great challenge to make a defects-free membrane. The metal-organic membranes (MOF) have advantages over polymeric membranes [16]. The metal cluster improved the porosity and stability significantly [10,12,17]. In MOF, both organic and inorganic building blocks are present. The organic ligands clinch to metal ion clusters. Mixed matrix membranes (MMM) have wonderful permeability and selectivity due to the inorganic fillers, which have naturally excellent separation properties [16,18–23]. In this research, an efficient metal-organic framework-based MMM was made to separate CO_2 from different gas mixtures.

Materials and Methods

All the chemicals used in the current study were of analytical grade. The chemicals utilized for MMMs development are Adenine, Cobalt acetate tetrahydrate, obtained from Alfa Aesar chemicals (Germany). Polyether sulfone (PES), N, N-dimethyl formamide (DMF), Methanol, and Chloroform were achieved by Fisher Scientific (USA). CH_4, CO_2, N_2 were purchased by Linde Chemicals (Germany) and used as such without any further purification.

Synthesis of Bio-MOF-11

Bio-MOF-11 was prepared according to the method described in the literature [20], with some minor changes. An amount of 1.30 g of adenine was mixed in 100 mL of DMF. 2.50 g of cobalt acetate was mixed in 100 mL of DMF. Both the solutions were ultra-sonicated and heated to homogenize the solution. A 75 mL stock solution of adenine and 25 mL stock solution of cobalt acetate solution, with a ratio of 3:1, were mixed and stirred well. The solution obtained was placed in the autoclave oven and heated at 120 °C, and later the solution was cooled at room temperature. The product obtained had purple octahedral crystals. This product was washed and centrifuged three times with DMF. The product was further washed three times with methanol and dried.

Synthesis of PES Membrane

To cast the PES membrane, PES was heated in a vacuum oven at a temperature of

110±5 ℃ overnight. Neat polymer and chloroform 20 mL were laced in a homogenizer. It was stirred for 24 h and then stored in a glass bottle. A smooth flat Petri dish was used to cast a membrane with an inverted funnel placed on it. The casted membrane was moved to an oven to remove the excess solvent. The membrane was heated at the temperature range 90-160 °C with a ramp of 5 °C/h. The resulting membrane was gradually cooled to room temperature.

MMM preparation

The material was dried in an oven at 105±5 °C for 24 h. An amount of 1 g of dried Bio-MOF-11 was mixed with chloroform, and it was stirred to prepare 10%, 20%, and 30% by wt. MOF suspension as per equation 1.

$$\text{Filter loading (Weight \%)} = \frac{\text{Weight of filler}}{\text{Weight of polymer} + \text{weight of filler}} \times 100 \quad (1)$$

The polymer solution was prepared according to the required amounts by following the Priming method. The solution of polymer was added gradually into MOF solution. Initially, 10% of the overall required amount of polymer solution was added into MOF solution. After 2 h, 10% remaining of the polymer solution was mixed into the finishing solution till the complete polymer solution was dissolved into MOF solution. The same procedure was repeated for other samples. Sample membranes were remained in an oven at 110 ±5 ℃ for 24 h and later characterized. A process flowchart is shown in Fig. 1(a).

MOFs Characterization

The synthesized Bio-MOF-11 was characterized by different instruments, which include Scanning electron microscopy (SEM) (Neon Zeiss), Thermal gravimetric-differential scanning calorimetry (TG-DSC, TGA/DSC1 STARe system from Mettler-Toledo), Fourier transform infrared spectroscopy (FTIR) by Perkin Elmer's Spectrum 100-FTIR, X-ray diffraction (XRD) by Bruker D8, Co Ka irradiation.

Permeation experiments

To check the performance of gas separation of mixed matrix membrane, a specially constructed gas permeation system, as shown in Figure 1(b) was used. The efficiency was calculated based on different parameters, i.e., temperature 25 – 55°C, feed flow rate 1 L/min, and pressure 10 bar, respectively. To place the membrane in the equipment, a porous metallic plate was used. It was sealed tightly with Viton O-ring. Retentate and permeate composition was analyzed by a gas chromatograph (YL Instrument, South Korea). All tests were performed in triplicate. In an auxiliary cylinder, the gas was expanded, and the pressure transducer took the reading of the rate of pressure increment.
Equation 2 tells us the calculation of gas permeability (P).

$$p = \frac{273 \times 10}{760} \times \frac{yiv}{AT\left[\frac{76}{14}.7\right]x_i P_2} \times \left[\frac{dp}{dt}\right] \quad (2)$$

Where, T = Temperature (K), P_2 = Feed gas Pressure (psi), V = Volume (cm^3) of Down Stream, A = permeation area (cm^2) of Membrane, y_i. = mole fractions of component i in downstream, x_i = mole fractions of component i in upstream.

The transportation of gases through Mixed Matrix Membranes uses the 'solution-diffusion' transport Method described in Equation 3.

$$P = D \times S \quad (3)$$

Where, P = Permeability, D = Diffusion coefficient, S=Solubility coefficient of gas in membrane phase.

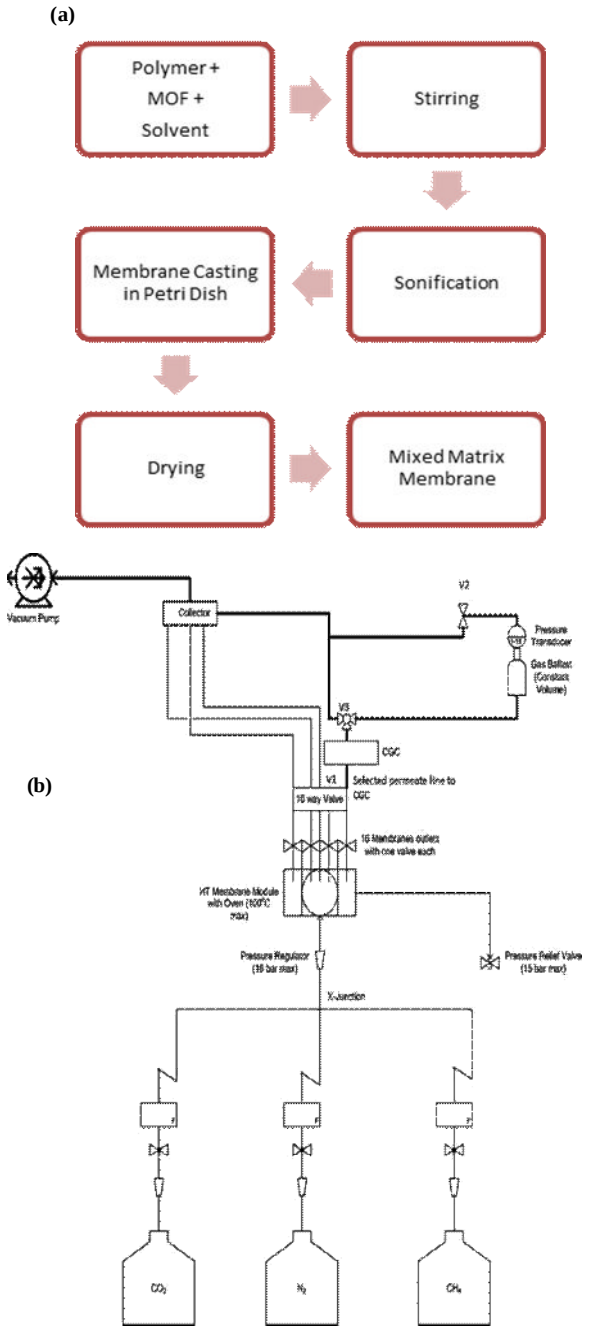

Figure 1. **(a) Process Flow Chart (b) Gas Permeation Setup**

To find out the diffusion coefficient of the membrane, the 'Time lag Method' was used. The above expression was also used to find out the solubility coefficient.

Equation 4 was used to calculate mixed-gas selectivity.

$$\alpha_{ij} = \frac{y_i / y_j}{x_i / x_j} \quad (4)$$

Where, x_j = Component Mole fraction j in upstream, x_i = Component Mole fraction 'i' in upstream, y_j = Component Mole fraction j in downstream, y_i = Component Mole fraction 'i' in downstream.

Results and Discussion

FTIR

FTIR spectra of the membrane were recorded in a wavelength range of 640 to 4000 cm^{-1} shown in Fig. 2 (a). It confirms the linkage of adenine, Co, and the functional group present in MOFs. We can see the adenine linkers and metal nodes linkage.

From the figure, we can see the two band peaks at the range of 665 and 870, which is the fingerprint profile shows CO-O stretching vibration. At 3330 cm^{-1} the characteristic peaks show N-H in adenine amine stretching. Similarly, at 1400-1605 cm^{-1} the bands represent the bending and stretching modes of the imidazole ring of adenine. The stronger peak on 1590 cm^{-1} represents the existence of C-N bending. At 900 to 1170 cm^{-1} shows C-H stretching in the structure of adenine.

XRD

The XRD with a particle size 150 microns was recorded at 2θ from 5 to 70° to find Bio-MOF-11 Co crystallinity. The pattern of XRD is the same as reported in the previous studies with the synthesis of bio-MOF-11 shown in Figure 2(b) [24]. Crystal size was found by using the Scherer equation, which is 6 nm given below:

$$L = \frac{k\lambda}{\beta}\cos\theta$$

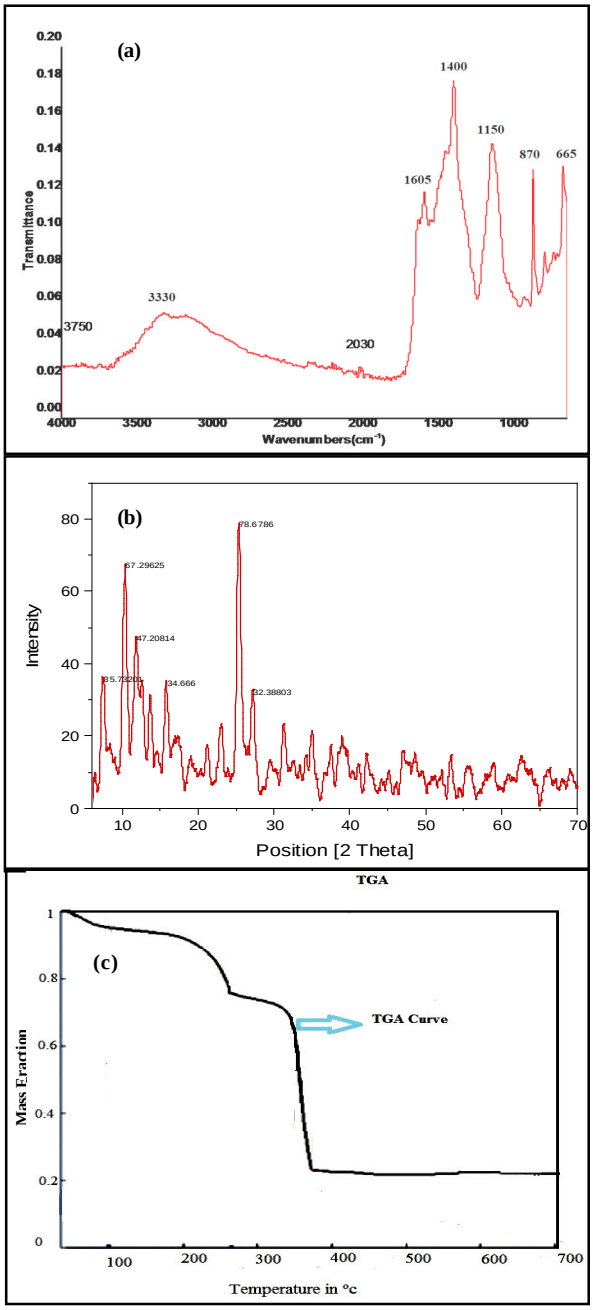

Figure 2. **Characterization of Bio MOF-11 (a) FTIR (b) XRD (c) TGA**

TGA

The study of Bio-MOF-11 -Co was also done by Thermogravimetric analysis (TGA) with the range of temperature 40°C to 700°C shown in Fig. 2(c). The environment was air which has a flow rate of 70 mL/min. It shows Metal-Organic Framework thermal stability with temperature. We can see in the figure that up to 110°C, weakly attached surface solvent/moisture was removed. At 110°C to 270°C, the bonded solvent molecule of DMF in the structure was removed. When the temperature touches 271°C, the organic linker's degradation started, and the complete structure was destroyed at 370 °C.

The glass transition temperature (GTT) is the temperature at which the carbon chain starts to leave its position. The higher the GTT value higher will be the stiffness and rigidity. It was seen that GTT increases with an increase in the concentration of Bio-MOF-11 in polyether sulfone (Fig. 3). The neat polyether sulfone has a GTT value of 220 °C which increases to 235 at 30% loading filler. The increase in GTT value of polyether sulfone with Bio-MOF-11 shows the improvement in toughness and strictness in MMM, the enhancement also showed the strong attraction between poly ether sulfone and Bio-MOF-11. A major cause of this enhancement of GTT measurement is that the filler particles are strongly surrounded by a polymer chain. Another reason is the improvement in the interlinking bond between the filler and polymer [23]. The GTT graph is shown in Fig. 3.

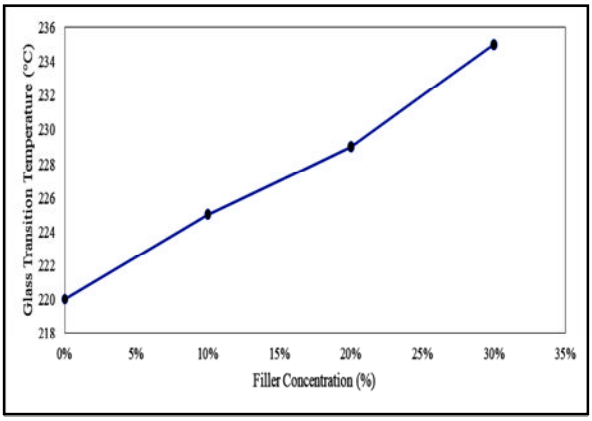

Figure 3. **Glass Transition Temperature of PES/Bio-MOF-11**

SEM

SEM presents a nano-sized crystal of Bio-MOF-11. They look like disc that was grown in shape like cauliflower. The morphology of Bio-MOF 11 is shown in Fig. 4(a) & (b), which showed highly ordered octahedral MOF particles of synthesized Bio-MOF-11. The reason is the post synthesized modification before fabricating MMM.

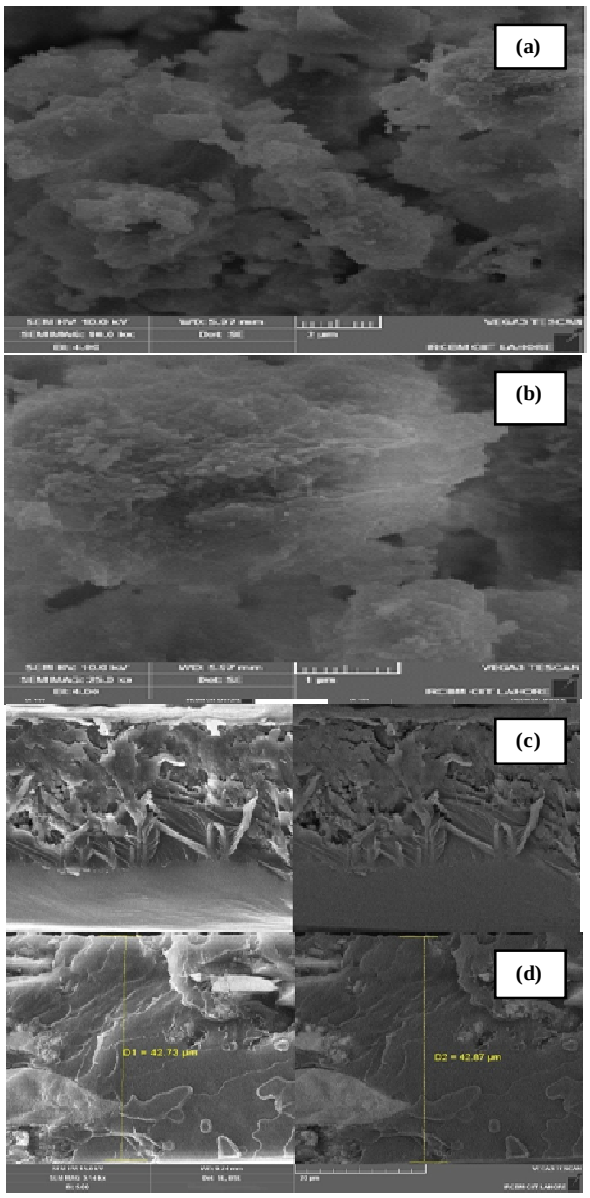

Figure 4. **(a) SEM of Bio-MOF11 at 2 µm. (b) SEM of Bio-MOF11 at 1 µm. (c) & (d) Morphology of Mixed Matrix Membrane)**

A scanning electron microscope was also used to find out the morphology of the mixed matrix membrane of Polyether sulphone and Bio MOF-11. The images are shown in Fig. 4(c) & (d). The images show that polyether sulphone and Bio MOF-11 particles have good interfacial adhesion. The images show no void among PES and MOF particles. The images also clearly show that the MOF particles are dispersed throughout the membrane homogeneously, proving that the polymer and MOF have solid interfacial interaction.

Gas Separation Performance

CO_2, N_2, and CH_4 gases were used at a pressure of 10 bar and a temperature of 25°C for measuring the permeability. Three coupons were separated from every membrane and examined at a gas permeation setup. Furthermore, the permeability of every coupon was examined three times and the average outcomes were utilized for analysis with error bars. Pure gas permeation results for CO_2/N_2 and CO_2/CH_4 gas pairs are shown in Fig. 5.

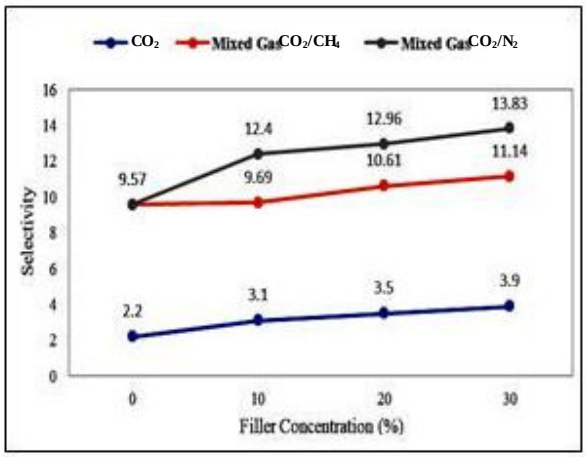

Figure 5. **Pure Gas Selectivity and Permeability Data of PES/Bio-MOF-11**

The incorporation of Bio-MOF-11 particle caused improvement in selectivity from 14.67 to 15 with different loading of

filler (0-30%) in CO_2/CH_4 pure gas. The slightly lower selectivity in 20% load filler may be due to the pore blockage. Similarly, it also improves the ideal selectivity of CO_2/ N_2 from 9.57 to 11.47 with a range of 0% to 30% loading of filler. The permeability of CO_2 also increases with the incorporation of Bio-MOF 11. The value of permeability jumps from 2.20 to 3.90. It was also observed that the selectivity of CO_2/CH_4 increases by 2.24% with the loading of filler 0 to 30%. Similarly, the permeability of CO_2 increases by 290% with filler loading ranges from 0-30% and the selectivity of CO_2/ N_2 increases by 19.85%.

Higher permeability of CO_2 will be attained if the % concentration of loading filler in poly ether sulfone is increased because Bio-MOF-11 has a higher affinity toward the molecules of CO_2. The CO_2 shows a higher quadrupole moment and displays a greater solubility coefficient when it is compared with nitrogen and methane which are nonpolar. In MMM, the solubility and diffusion coefficient determination of CO_2 can give the gas separation performance. The solubility, diffusivity, and permeability of CO_2 are displayed in Fig. 6.

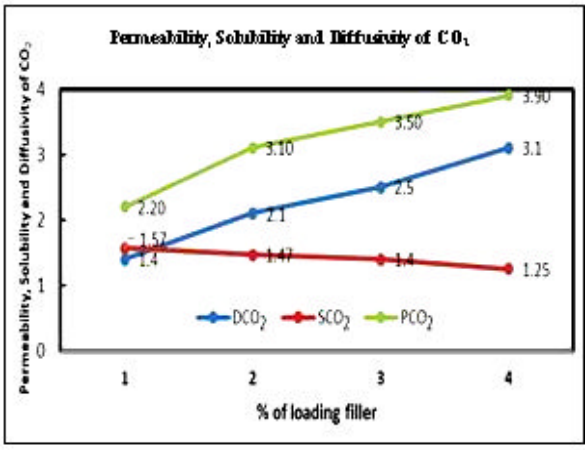

Figure 6. **Permeability, Solubility, and Diffusivity of CO_2**

It is seen that the permeability of CO_2 is increasing with increasing filler concentration. It also observed that the diffusion of CO_2 is increasing while the solubility is decreasing. The reason for increasing diffusion is the adenine structural units Lewis basic site present in Bio-MOF-11, which has stronger CO_2 molecule adsorption ability, causing better diffusion. The diffusion has inverse proportionality with solubility so when diffusion increases, then automatically solubility decreases. The MMM was also examined for gas permeation performance in pairs of gases, i.e., CO_2/N_2 and CO_2/CH_4. The outcomes are represented in Fig. 7 (a) & (b) in mixed gas conditions.

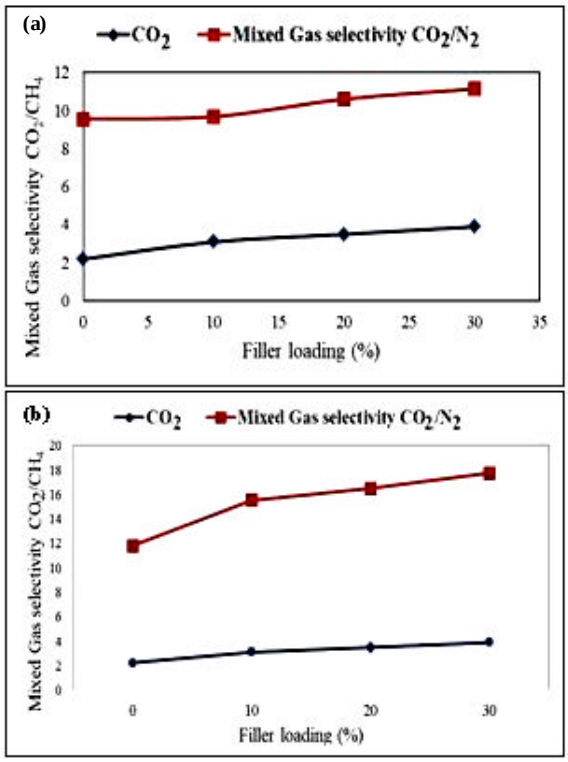

Figure 7. **(a) CO_2/N_2 Selectivity and Permeability Data of PES/Bio-MOF-11; (b) CO_2/CH_4 Selectivity and Permeability Data of PES/Bio-MOF-11)**

The permeability of pure gas is greater than the permeability of mixed gas. The reason is the phenomenon of gas molecule competitive sorption. The permeability of CO_2 has slowed down with the molecules of N_2 and CH_4 gases existence because they have greater

kinetic diameter than CO_2. The CO_2 also leads to polymer matrix plasticization because the CO_2 gas is condensable. This also affects the selectivity of the membrane, which later decreases. At partial pressure of 5 bar, the behavior of CO_2 gas was checked for MMM in a mixed gas condition which was less than the plasticization pressure of PES. So, selectivity difference is ascribed to competitive sorption.

Effect of Operating Temperature on Memerane Performance

The overall permeability was increased at higher temperatures in MMMs, as shown in Fig. 8. With an increase in the temperature of the MMM the permeability of CO_2 increases. The enhancement of CO_2 permeability at higher temperatures is due to the polymer gaining a property, and it becomes flexible, resulting in free volumes that lead to a reduction in selectivity but enhanced gas permeability.

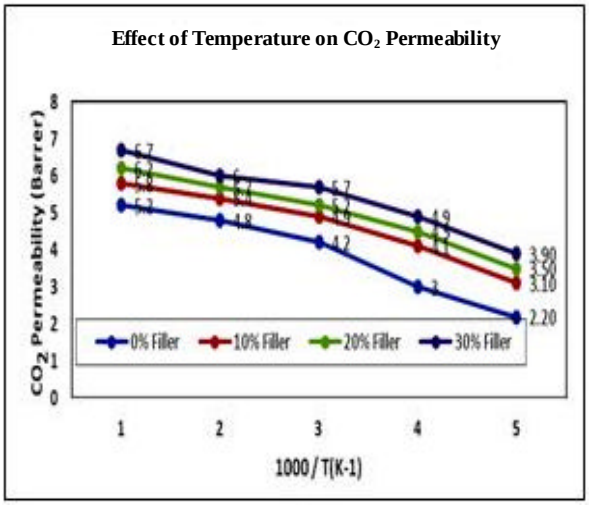

Arrhenius equation gives us permeation activation energy (E_p), and operating feed temperature, permeability.

$$P = P_o \exp\left(\frac{-EP}{RT}\right) \quad (5)$$

T= Feed Temperature Absolute.
P_o = Pre exponential factor.
R =Gas constant,
P= Permeability of Gas.

The values for activation energies of permeation for CO_2 were calculated and presented in Fig. 9(a).

The activation energy of Permeation = sorption Heat + Diffusion Activation Energy.

$$E_P = H_S + E_D \quad (6)$$

The activation energy of permeation tells us how much a gas molecule shows confrontation when it passes through the MMM. If the value of activation energy is low, then it is expected that the permeability of gas will be higher. If the activation energy value is higher than the permeability of gas through a MMM will below. In this study, the activation energy of CO_2 decreased with increasing the percent of loading filler (Bio-MOF-11). It shows that with increasing temperature, CO_2 permeability will increase; it also proves that polymer and filler are incorporating with each other and sharing the properties.

The developed Bio-MOF-11 incorporated MMM showed a good separation result. To bring more precision, the performance was compared with the reported literature. For this purpose, Roberson's upper bound trade-off plot was drafted, as shown in Fig. 9(b). It is shown in the figure that as the concentration of filler increases the result came nearer to the upper bound which proves that it can be one of the potential candidates for the separation of CO_2.

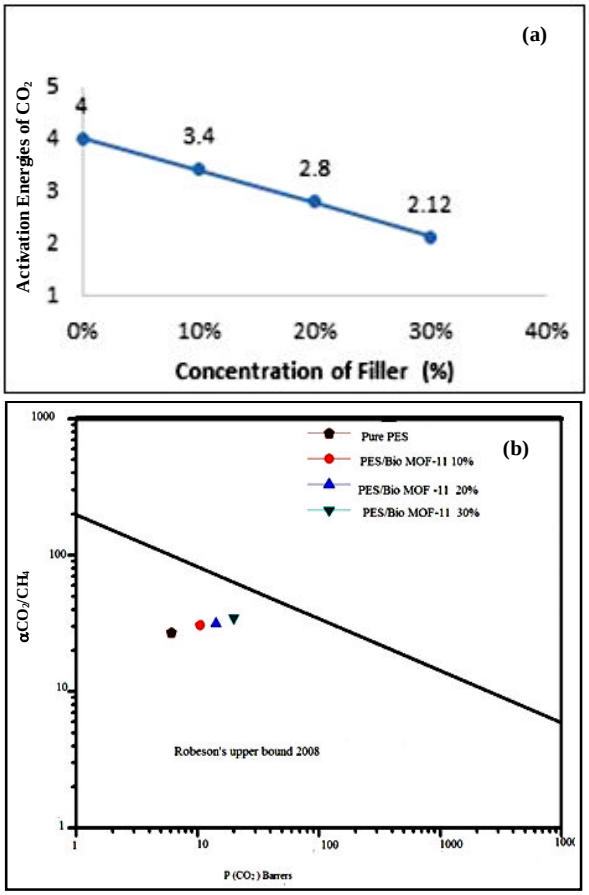

Figure 9. **(a) Activation Energy of PES/Bio –MOF-11; (b) Comparison of gas separation performance for pure PES and different filler**

Conclusion

In this study, adenine and cobalt-based Bio-MOF-11 were synthesized, characterized, and mixed with polyether sulfone to cast membrane. The results of FTIR, XRD, and SEM images show a good combination between cobalt and adenine. This membrane was tested for CO_2 separation from the mixture of CO_2, CH_4, and N_2. In the start, the permeability and selectivity were tested for pure gases and then for a mixture of gasses that have 50/50 concentration. The results showed that increasing filler concentration, the permeability of CO_2 increases. The selectivity of CO_2/CH_4 and CO_2/N_2 also increases. The separation performance was close to the Robeson upper bound, which shows that it can be an ideal candidate for the separation of CO_2.

Acknowledgement

The authors are grateful for the laboratory facilities provided by the Department of Chemical Engineering, University of Gujrat, Pakistan, and the Membrane Technology Lab, COMSATS Lahore Campus. We also appreciate the Department of Chemical Engineering at BUITEMS Quetta, Pakistan, for providing a workspace and IT support that enabled us to complete this manuscript on time. Furthermore, we appreciate the positive feedback from reviewers, which helped us improve the quality of our work.

Conflict of Interest

The authors declare no conflict of interest to disclose.

References

1. Z. N. Qaisrani, S. Shams, Z. Guo and A. A. Mamun, *Pollution*, 6 (2020) 569. https://dx.doi.org/10.22059/poll.2020.297713.751
2. Z. N. Qaisrani, N. Nuthammachot, K. Techato, Asadullah, G. H. Jatoi, B. Mahmood and R. Ahmed, *Braz. J. Biol.*, 84 (2022) 12. https://doi.org/10.1590/1519-6984. 261001
3. Z. N. Qaisrani, S. Shams, G. Zhenren, MS. Reza and Q. Zaunuddin, *IET Digit. Lib.*, (2018) 4. https://doi.org/10.1049/cp.2018.1605
4. J. An, S. J. Geib and N. L. Rosi. *Am. J. Chem. Soc. Commun.*, 132 (2009) 38. https://doi.org/10.1021/ja909169x
5. M. Siddique, S. A. Soomro, Z. N. Qaisrani, A. S. Jatoi, Asadullah, G. Khan and E. Kakar, *Pak. J. Anal. Environ. Chem.*, 17 (2016) 18.

10.21743/pjaec/2016.06.003
6. D. Aaron and C. Tsouris, *Sep. Sci. Technol.*, 40 (2011) 321. https://doi.org/10.1081/SS-200042244
7. G. Myhre, O. Boucher, F. Bréon, P. Forster and D. Shindell, *Nat. Geosci.*, 8 (2015) 181. https://doi.org/10.1038/ngeo2371
8. K. Sumida, D. L. Rogow, J. A. Mason, T. M. Mcdonald, E. D. Bloch, Z. R. Herm, T. H. Bae and J. R. Long, *Chem. Rev.*, 112 (2012) 724. https://doi.org/10.1021/cr2003272
9. J. Lehmann, *Commentary*, 447 (2007) 143. https://doi.org/10.1038/447143a
10. T. Li, J. E. Sullivan and N. L. Rosi, *J. Am. Chem. Soc.*, 135 (2013) 9984. https://doi.org/10.1021/ja403008j
11. M. R. Azhar, P. Vijay, M. O. Tade, H. Sun and S. Wang, *Chemosphere*, 196 (2017) 105. https://doi.org/10.1016/j.chemosphere.2017.12.164
12. Z. Tahir, A. Ilyas, X. Li, MR. Bilad and I. F. J. Vankelecom, *J. Appl. Polym. Sci.*, (2017) 45952. https://doi.org/10.1002/app.45952
13. Z. Tahir, M. Aslam, M. Amjad and M. Roil. *Sep. Purif. Technol.*, 224 (2019) 524. https://doi.org/10.1016/j.seppur.2019.05.060
14. I. Erucar and S. Keskin. *Chem. Eng. Sci.*, 130 (2015) 120. https://doi.org/10.1016/j.ces.2015.03.016
15. M. Rizwan, H. Rasool, H. Sun, V. Periasamy, MO. Tadé and S. Wang, *J. Colloid Interface Sci.*, 490 (2017) 685. https://doi.org/10.1016/j.jcis.2016.11.100
16. H. Asghar, A. Ilyas, Z. Tahir, X. Li and A.L. Khan, *Sep. Purif. Technol.*, 203 (2018) 233. https://doi.org/10.1016/j.seppur.2018.04.047
17. J. Dechnik, C. J. Sumby and C. Janiak, *Cryst. Growth Des.*, 17 (2017) 4467. https://doi.org/10.1021/acs.cgd.7b00595
18. T. Li, D-L. Chen, J. E. Sullivan, M. T. Kozlowski, J. K. Johnson and N. L. Rosi, *Chem. Sci.*, 4 (2013) 1746. http://dx.doi.org/10.1039/C3SC22207A
19. M. W. Anjum, F. Vermoortele, A. L. Khan, B. Bueken, D. D. Vos and I. F. J. Vankelecom, *ACS Appl. Mater. Interfacts*, 7 (2015) 25193. https://doi.org/10.1021/acsami.5b08964
20. S. Ishaq, R. Tamime, M. R. Bilad and A. L. Khan, *Sep. Purif. Technol.*, 210 (2018) 442. https://doi.org/10.1016/j.seppur.2018.08.031
23. M. W. Anjum, B. Bueken, D. D. Vos, I. F. J. Vankelecom, *J. Memb. Sci.*, 125 (2015) 21. https://doi.org/10.1016/j.memsci.2015.12.022
24. S. Shah, H. Sheikh, S. Hafeez and M. I. Malik. *Pak. J. Anal. Environ. Chem.*, 21 (2020) 44. http://doi.org/10.21743/pjaec/2020.06.06